Iva Blazkova[1]
Hoai Viet Nguyen[1]
Marketa Kominkova[1]
Romana Konecna[1]
Dagmar Chudobova[1]
Ludmila Krejcova[1,2]
Pavel Kopel[1,2]
David Hynek[1,2]
Ondrej Zitka[1,2,3]
Miroslava Beklova[2,3]
Vojtech Adam[1,2]
Rene Kizek[1,2]

[1]Faculty of Agronomy, Department of Chemistry and Biochemistry, Mendel University in Brno, Brno, Czech Republic
[2]Central European Institute of Technology, Brno University of Technology, Brno, Czech Republic
[3]Faculty of Veterinary Hygiene and Ecology, Department of Veterinary Ecology and Environmental Protection, University of Veterinary and Pharmaceutical Sciences, Brno, Czech Republic

Received August 15, 2013
Revised November 5, 2013
Accepted November 5, 2013

Research Article

Fullerene as a transporter for doxorubicin investigated by analytical methods and in vivo imaging

Carbon nanomaterials, including fullerenes, exhibit not only unique structure and electronic properties but also a significant potential to serve as radical scavengers and/or anti-oxidants. Their conjugation with anticancer drugs such as doxorubicin (DOX) may help to balance severe negative side effects of these cytostatics and also improve the delivery of the drug taking advantage of the enhanced cellular uptake, selectivity to cancer cells, and pH regulated release. In this study, the fullerene (C60) surface was oxidized by concentrated nitric acid, which enabled simple DOX–fullerene conjugation based on π–π stacking and hydrophilic interactions with carboxylic groups. The strength of this noncovalent binding is pH dependent. At a low pH, the amino group of DOX is protonated, however at a higher pH, the amino group is deprotonated, resulting in stronger hydrophobic interactions with the fullerene walls. CE and HPLC were employed for characterization of resulting complexes. The cell toxicity of the conjugates was evaluated using *Staphylococcus aureus* and finally they were administered into the chicken embryo to assess the applicability for in vivo imaging.

Keywords:
Clinical analysis / Doxorubicin / Drug delivery / Embryo / Fullerene / Nanomedicine
DOI 10.1002/elps.201300393

1 Introduction

Nanomaterials are nowadays attracting enormous attention in almost all research areas. Hence there is no wonder that their application in medicine is so widely explored. Both, diagnostic as well as therapeutic utilization of various types of nanoparticles have been investigated [1–4]. Metal or semiconductor nanoparticles are employed for imaging applications and visualization, and magnetic particles are utilized for hyperthermia therapy, and variety of other types of nanomaterials are used for drug delivering. Prominent position among nanomaterials used in medicine belongs to carbon nanomaterials such as nanotubes, fullerenes, and/or graphene due to their unique physical and chemical properties [1–3, 5–7]. The π–π stacking effect can be utilized for conjugation of aromatic molecules onto the polyaromatic surface of all carbon nanomaterials. Moreover, fullerenes and their derivatives were studied for their efficient quenching of various free radicals and reactive oxygen species, thus potentially serving as radical scavengers and/or anti-oxidants in biological systems protecting from the oxidative stress and toxicity caused by cytostatic drugs [8–11]. The combination of the protective properties of fullerenes and their ability of drug delivery make them very attractive for anticancer therapy [12,13]. For the clinically highly effective anticancer drug paclitaxel, it was shown that covalent conjugate with C60 for a lipophilic slow-release system enhanced the therapeutic efficacy [14]. Doxorubicin (DOX), another highly effective cytostatic drug in antitumor therapy [15], was also conjugated with fullerenes and carbon nanotubes aiming at mitigating DOX-induced toxic side effects [8, 16, 17] and/or improving the drug delivery [18–21]. Moreover, the optical properties of DOX provide opportunities to track the molecules and conjugates by using fluorescence-based techniques, such as assessing nanocarrier of DOX in cells without any other fluorescence labels [22]. Generally, the coupling between DOX and fullerene surface can be assured by covalent linkage [13, 23], or by nonspecific interaction after activation of the surface by acidic oxidation [18].

In this study, the simple method of DOX–fullerene (C60) conjugation is utilized and the characterization of conjugates by spectral methods, electrochemical analysis, CE, and LC is

Correspondence: Dr. Rene Kizek, Department of Chemistry and Biochemistry, Mendel University in Brno, Zemedelska 1, CZ-613 00 Brno, Czech Republic
E-mail: kizek@sci.muni.cz
Fax: +420-5-4521-2044

Abbreviation: DOX, doxorubicin; **ED**, electrochemical detection; **IC_{50}**, half maximal inhibitory concentration

Colour Online: See the article online to view Figs. 1–6 in colour.

demonstrated. Finally, the monitoring of the effect of prepared conjugates on the bacterial cells as well as in vivo imaging on the chicken embryo is presented.

2 Materials and methods

2.1 Chemicals and pH measurement

HPLC-grade ACN (>99.9%; v/v) from Merck (Darmstadt, Germany) was used. Chemicals used in this study were purchased from Sigma-Aldrich® (St. Louis, MO, USA) in ACS purity unless noted otherwise. Washing solutions were prepared in MilliQ water obtained using reverse osmosis equipment Aqual 25 (Aqual, Brno, Czech Republic). The DI water was further purified by using apparatus Direct-Q 3 UV Water Purification System equipped with the UV lamp from Millipore (Billerica, MA, USA). The resistance was established to 18 MΩ/cm. The pH was measured using pH meter WTW inoLab (Weilheim, Germany).

2.2 Synthesis of the fullerenes with DOX

2.2.1 Conjugates with constant concentration of fullerenes and varying concentration of DOX

The Buckminster Fullerenes C60 (5 mg; Sigma-Aldrich®) were purified with concentrated HNO_3 (70% in ACS water, 1 mL) for 15 min in ultrasonic bath and shaken (1400 rpm, 90°C, 15 min, Thermomixer® comfort, Eppendorf, Germany). The solution was centrifuged (25 000 × *g*, 20°C, 15 min; Centrifuge 5417R, Eppendorf) and the acid was removed. The fullerenes were washed with 1 mL of ACS water (seven times) until the neutral pH was reached and finally resuspended in 1 mL of ACS water. Fifty microliters of the fullerene solution was mixed with 500 μL of the DOX (1000, 500, 250, 125, and 63 μg/ml in ACS water). The solution was sonicated in the ultrasonic bath for 15 min, after 5 min of sonication, 1 mL of the sodium phosphate buffer (pH 7.5) was added. The solution was vortexed for 24 h and subsequently centrifuged using Amicon 3 K (4500 × *g*, 20°C, 15 min; centrifugal filters for sample purification and concentration; EMD Millipore). The solution was subsequently washed with sodium phosphate buffer (pH 7.5) and centrifugation was repeated. Finally the solution of fullerenes and DOX was filled up to 1 mL by ACS water.

2.2.2 Conjugates with constant concentration of DOX and varying concentration of fullerenes

The different concentrations of fullerenes with DOX were prepared in the same way as previous method (Section 2.2.1). There were different fullerenes weight (2.5, 5, 7.5, 10, 12.5 mg) prepared and the one concentration of DOX as 500 μg/mL was used.

2.3 Antimicrobial effect

The procedure for the evaluation of the antimicrobial effect of the fullerenes, DOX, and DOX–fullerene conjugates was based on measuring the absorbance using the apparatus Multiskan EX (Thermo Fisher Scientific, Germany) and subsequent analysis in the form of growth curves. The bacterial culture of *Staphylococcus aureus* cultivated in LB medium (meat peptone 5 g/L, NaCl 5 g/L, bovine extract 1.5 g/L, yeast extract 1.5 g/L HIMEDIA, Mumbai, India; sterilized MilliQ water with 18 MΩ) was diluted with LB medium to absorbance 0.1 at a wavelength of 600 nm, measured using Specord spectrophotometer 210 (Analytik, Jena, Germany). The culture (250 μL) was mixed with different concentrations (1, 2, 4, 8, 16, 31, 63, 125, 250, or 500 μg/mL) of DOX in ACS water, fullerene, or fullerene with DOX. Measurements were carried out at time 0, then every 30 min for 24 h at 37°C and the wavelength of 600 nm.

2.4 Spectrometric characterization of DOX–fullerene conjugates

The absorbance and fluorescence scans of all solutions were acquired using a microtitration plate reader Tecan infinite M200 PRO (Grödig, Austria). A volume of 50 μL of the solution was analyzed in the Costar® microtitration plate (UV plate, 96 well; Corning, NY, USA). The absorbance scan was measured within the range from 230 to 800 nm. The fluorescence spectrum was measured using excitation wavelength 480 nm and emission range of 520–850 nm (emission wavelength step size: 5 nm; gain: 100; number of flashes: 5).

2.5 Electrochemical analysis

Determination of DOX and fullerene interaction by square wave voltammetry (SWV) was performed using a 663 VA Stand (Metrohm, Herisau, Switzerland), equipped with standard electrochemical cell and three electrodes. The three-electrode system consisted of a hanging mercury drop electrode (HMDE) with a drop area of 0.4 mm^2 as the working electrode, an Ag/AgCl/3M KCl reference electrode and a platinum electrode acting as the auxiliary electrode. GPES 4.9 software was employed for data processing. The analyzed samples were deoxygenated prior to measurements by purging with argon (99.999%). Acetate buffer (0.2 M CH_3COONa and CH_3COOH, pH 5.0) was used as a supporting electrolyte. The supporting electrolyte was replaced prior to each analysis. The parameters of the measurement were as follows: purging time 120 s; deposition potential 0.0 V; time of accumulation 120 s; equilibration time 2 s; initial potential 0.0 V; end potential −1.7 V; step potential 0.005 V; modulation amplitude 0.0250 V; volume of measurement cell 1 mL (5 μL of sample; 995 μL acetate buffer).

2.6 Ex vivo imaging

The DOX and the DOX with fullerenes were applied by injection into the chicken embryo breast muscle tissue. The fluorescence was detected by Carestream In-Vivo Xtreme Imaging System (Carestream Health, Rochester, USA). This instrument is equipped with a 400 W xenon light source. Emitted light was captured by a 4MP CCD camera. The excitation wavelength was set at 480 nm and the emission was measured at 600 nm. Other parameters were set as follows: exposure time 2 s; binning 2×2; *f*-stop 1.1; field of view 11.5 × 11.5 cm. The images were processed by Carestream molecular imaging software.

2.7 In vivo experiment

The in vivo distribution of the DOX with fullerene within a body was studied in the chicken embryos. The eggs (ISA Brown) were incubated in RCom 50 MAX incubator (Gyeongnam, Korea) at temperature (37.5°C) and humidity (45% rH) control and automatic egg rolling (every 2 h). There was 250 μL of the fullerene (5 mg/mL) with DOX (31, 63, 125, 250, 500 μg/mL) injected into egg yolk of five eggs with chicken embryo (17 days old). The eggs were incubated for 4 h at 37.5°C. After the incubation the eggshell was removed and the organs were sampled, homogenized, and analyzed by HPLC with electrochemical detection (HPLC-ED) according to the protocol described in the following sections.

2.8 HPLC analyses

2.8.1 Sample preparation

A tissue samples were ground in a mortar using liquid nitrogen with PBS. Samples were further disrupted using an ultrasonic needle. Subsequently, the samples were vortexed (5 min) and centrifuged (25 000 × *g*, 4°C, 20 min). TFA (5%, v/v) was added and the centrifugation was repeated at the same condition. The supernatant was used for the analysis of DOX using HPLC-ED.

2.8.2 HPLC analyses

The samples were analyzed using HPLC with electrochemical and UV-VIS detection (HPLC-ED or HPLC-UV). HPLC system consisted of two solvent delivery pumps operating in the range of 0.001–9.999 mL/min (Model 582 ESA and Model 584 ESA; ESA, Chelmsford, MA), with RP chromatographic colony Zorbax eclipse AAA C18 (150 × 4.6; 3.5 nm particles, Agilent Technologies, USA) and a Coulochem electrochemical detector. The electrochemical detector includes one low volume flow-through analytical cell (Model 5040, ESA, USA), which is consisted of glassy carbon working electrode, hydrogen–palladium electrode as reference electrode and auxiliary electrode, and Coulochem III as a control module. Both the detector and the reaction coil/column were thermostated. The absorbance detector LaChrom Elite L – 2420 with a single wavelength (485 nm) by Hitachi (Berkshire, United Kingdom) was employed.

The sample (20 μL) was injected using autosampler (Model 542 HPLC, ESA, USA). Samples were kept in the carousel at 8°C during the analysis. The column was thermostated at 30°C. The flow rate was 1 mL/min. Mobile phase consisted of: (i) aqueous solution of 0.05 M Na_2HPO_4 with 0.05% triethylamine (pH 4.6 was adjusted by citric acid) and (ii) ACN. The detection of the separated compounds was carried out at 400 mV. Analysis time was 20 min. Samples were diluted ten times prior to the analysis.

2.9 CE-LIF

Measurements were done by Beckman P/ACE MDQ CE (USA) with LIF detection (λ_{ex} = 488 nm, λ_{em} = 600 nm). Uncoated fused silica capillary (l_{tot} = 63.5 cm, l_{eff} = 54.5 cm, and id = 75 μm) was used. BGE was 100 mM phosphate buffer of pH 5.0 with 60 μM spermine and 70% of ACN v/v. Separation was carried out at 25 kV with hydrodynamic injection 15 s by 34 mbar. Samples were diluted 100 times prior to the analysis.

3 Results and discussion

Fullerenes and fullerenols have recently proved their suitability for transport of selected compound with therapeutic properties. The size of fullerenes improves the retention of the conjugated pharmaceutical drug in the organism and therefore prolongs the therapeutic activity of the drug. Previous studies have presented conjugation of fullerene and DOX via covalent bond to the specific linker, however nonspecific interactions between DOX and carbon nanotubes were described in the work by Heister et al. [18] taking advantage from the oxidation of the carbon material by nitric acid. Based on these results we subjected fullerenes to the same procedure (Fig. 1) and obtained product was characterized.

A set of solutions of (i) pure DOX in various concentrations, (ii) fullerenes in different concentrations, (iii) DOX–fullerene conjugates prepared using constant concentration of fullerenes and varying concentration of DOX, and (iv) DOX–fullerene conjugates using constant concentration of DOX and varying concentration of fullerenes was prepared.

3.1 The antimicrobial activity of DOX–fullerene conjugates

At first, the influence of all compounds on bacterial cells of *S. aureus* was observed to establish their suitability for biological application. The results expressed as growth curves can be seen in Fig. 2. One of the methods: how to demonstrate the antimicrobial activity of the studied compound is a

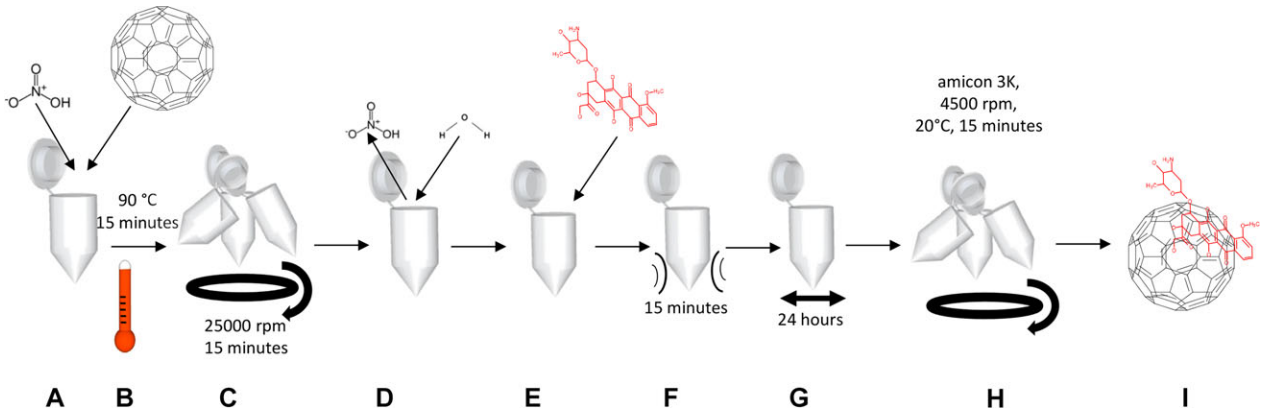

Figure 1. Scheme of preparation of DOX–fullerene conjugates. (A) Mixture of fullerenes and nitric acid, (B) heating for 15 min at 90°C, (C) centrifugation at 25 000 × *g* for 15 min, (D) replacing of nitric acid by water, (E) addition of DOX, (F) sonication for 15 min, (G) vortexing for 24 h, and (H) filtration using centrifugation filters (size 3 K, 4500 × *g* 15 min).

method of growth curves [24–26]. Using these curves and statistical methods it is possible to determine the IC_{50} value (half maximal inhibitory concentration) expressing the concentration required for 50% growth inhibition [27]. The growth of the culture exposed to the eleven concentrations of DOX (0, 1, 2, 4, 8, 16, 31, 63, 125, 250, and 500 μg/mL) is shown in Fig. 2A. Partial and total growth inhibition was observed when the concentrations of 4 and 31 μg/mL, respectively, were used. Application of the fullerene solutions to the *S. aureus* culture did not influence the cell growth as shown in Fig. 2B. In the case of exposure of the cell culture to the solutions of DOX–fullerene conjugates prepared by constant concentration of fullerenes and varying concentration of DOX, the total growth inhibition was not observed under any tested concentration (Fig. 2C). Even though the decrease of the growth curves was obvious it can be concluded that the antimicrobial effect of DOX is slightly suppressed by the presence of fullerenes. The largest influence of all tested solutions on the *S. aureus* culture was observed when solutions of DOX–fullerene conjugates prepared by constant concentration of DOX and varying concentration of fullerenes were applied (Fig. 2D). In this case, even the lowest fullerene concentration (2.5 mg/mL) caused the growth inhibition; however, the impact was not as lethal as in case of exposure to the pure DOX at the same concentration. The obtained results were verified by statistical calculations of IC_{50} values when the lowest value—2500 μg/mL (fullerene concentration) was determined for the last tested variant (Fig. 2D). Based on these results it can be concluded that fullerenes have a significant protective effect against DOX toxicity because for pure DOX solution the IC_{50} is only 15.1 μg/mL.

3.2 Spectroscopic properties of DOX–fullerene conjugates

The promising results obtained using *S. aureus* cultures were encouraging for further investigation of the properties of the DOX–fullerene conjugates. Spectroscopic characterization is shown in Fig. 3. The absorption spectra of conjugates prepared using constant concentration of fullerenes and increasing concentration of DOX exhibit strong signal in the ultraviolet range, and a band with the maximum at 480 nm was observed (Fig. 3A). These signals belong to the DOX molecules adsorbed on the fullerene molecules. Due to the fluorescence properties of DOX, also DOX–fullerene conjugates can be analyzed by fluorescence spectrometry. The intensive maximum of fluorescence emission of the conjugates was detected at 600 nm (Fig. 3B), which is the same wavelength as the emission maximum of DOX solution. Significant quenching of fluorescence was observed depending on the increasing concentration of DOX utilized for preparation of DOX–fullerene conjugates. The fluorescence intensities at 600 nm depending on DOX concentration are plotted in the inset in Fig. 3B. The comparison of the fluorescence intensity of DOX solution and solutions of DOX–fullerene conjugates in the linear range revealed that 47.8% of DOX employed for conjugate preparation was retained and adsorbed to surface of the fullerene molecules.

3.3 Electrochemical properties of DOX–fullerene conjugates

Besides optical, also electrochemical characterization of prepared conjugates was performed (Fig. 3C and D). Using square wave voltammetry, it was observed that DOX solution provided one peak at the potential of −0.47 V (data not shown but correspond to the literature [28–32]), however, when DOX–fullerene conjugates were prepared, the signal changed significantly. Two peaks were observed with maxima at potentials of −0.47 V and −0.51 V. The voltammograms for DOX–fullerenes prepared using constant concentration of fullerenes and varying concentration of DOX (8, 16, 31, 63, 125, 250, and 500 μg/mL) are shown in Fig. 3C. In three lowest concentrations of DOX (8, 16, and 31 μg/mL) the signal was below LOD of the method. For the remaining DOX concentrations (63, 125, 250, and 500 μg/mL), the sum peak area was plotted versus DOX concentration applied for the

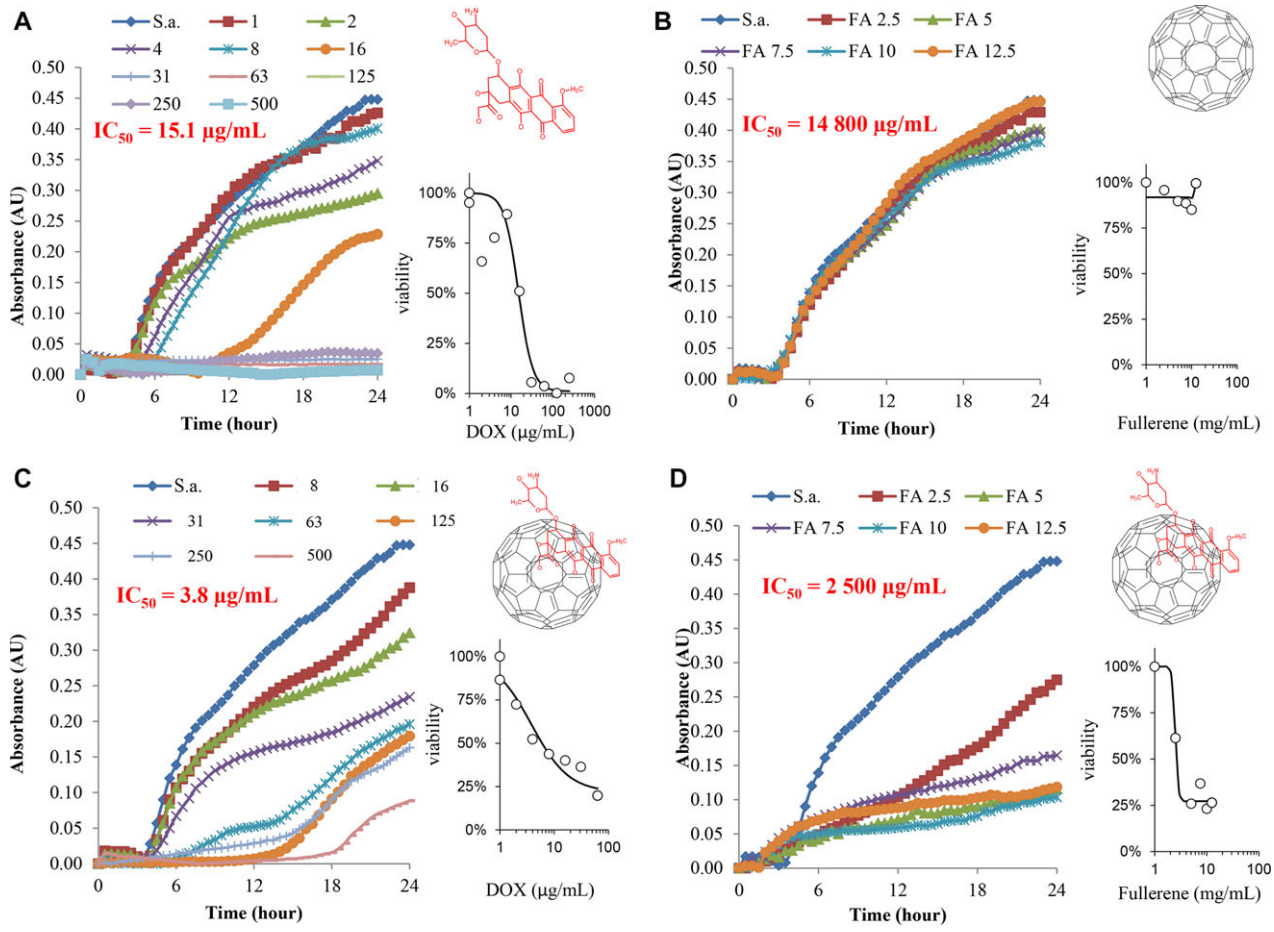

Figure 2. Growth curves of *S. aureus* cultivated in the presence of (A) DOX (0, 1, 2, 4, 8, 16, 31, 63, 125, 250, and 500 µg/mL), (B) fullerenes (0, 2.5, 5, 7.5, 10, and 12.5 mg/mL), (C) conjugates prepared using constant concentration of fullerenes (5 mg/mL) and varying concentration of DOX (0, 8, 16, 31, 63, 125, 250, and 500 µg/mL), and (D) solution prepared using constant concentration of DOX (500 µg/mL) and varying concentration of fullerenes (0, 2.5, 5, 7.5, 10, 12.5 mg/mL). The IC_{50} values were determined for 24 h of influence.

preparation process and a linear trend was observed as shown in the inset in Fig. 3C. The sum peak area was evaluated because it is the most general and suitable method for quantification of such record. The peak height of individual peaks is changing with the changing DOX concentration. The peak 1 height grows with increasing DOX concentration unlike the decreasing peak 2 height.

In the case of the DOX–fullerene conjugates prepared using the constant concentration of DOX and varying concentration of fullerenes the opposite trend was observed, even though the pure fullerene solution is electrochemically inactive and does not provide any peak at the observed potential range. In this place it is necessary to note that electrochemical inactivation of fullerene is connected with the detection method presented here. On the contrary, application of fullerene in the electrochemical research is very widespread [33–36]. The conjugation of DOX with fullerenes caused of the significant decrease of both peaks depending on the increasing amount of fullerene used for the DOX–fullerene conjugation process. The voltammograms are shown in Fig. 3D and as shown in the inset of this figure, the sum peak area is linearly dependent on the concentration of employed fullerenes. This behavior can be explained by the fact that the increasing amount of fullerenes in the solution act as the electronic insulator and prevent the transport of electrons between electrode and DOX molecules.

3.4 HPLC and CE characterization of DOX–fullerene conjugates

The adsorption of DOX molecules on the fullerene molecules leads to the formation of numerous complexes with various stechiometries, which cannot be revealed by stationary analyses and therefore separation techniques including HPLC and CE were employed.

To gain more information about properties of prepared conjugates three different detection techniques were utilized: HPLC-UV, HPLC-ED, and CE-LIF. The results for the set of conjugates prepared using constant concentration of fullerenes and increasing concentration of DOX are shown in Fig. 4. It was found that the retention time of DOX was

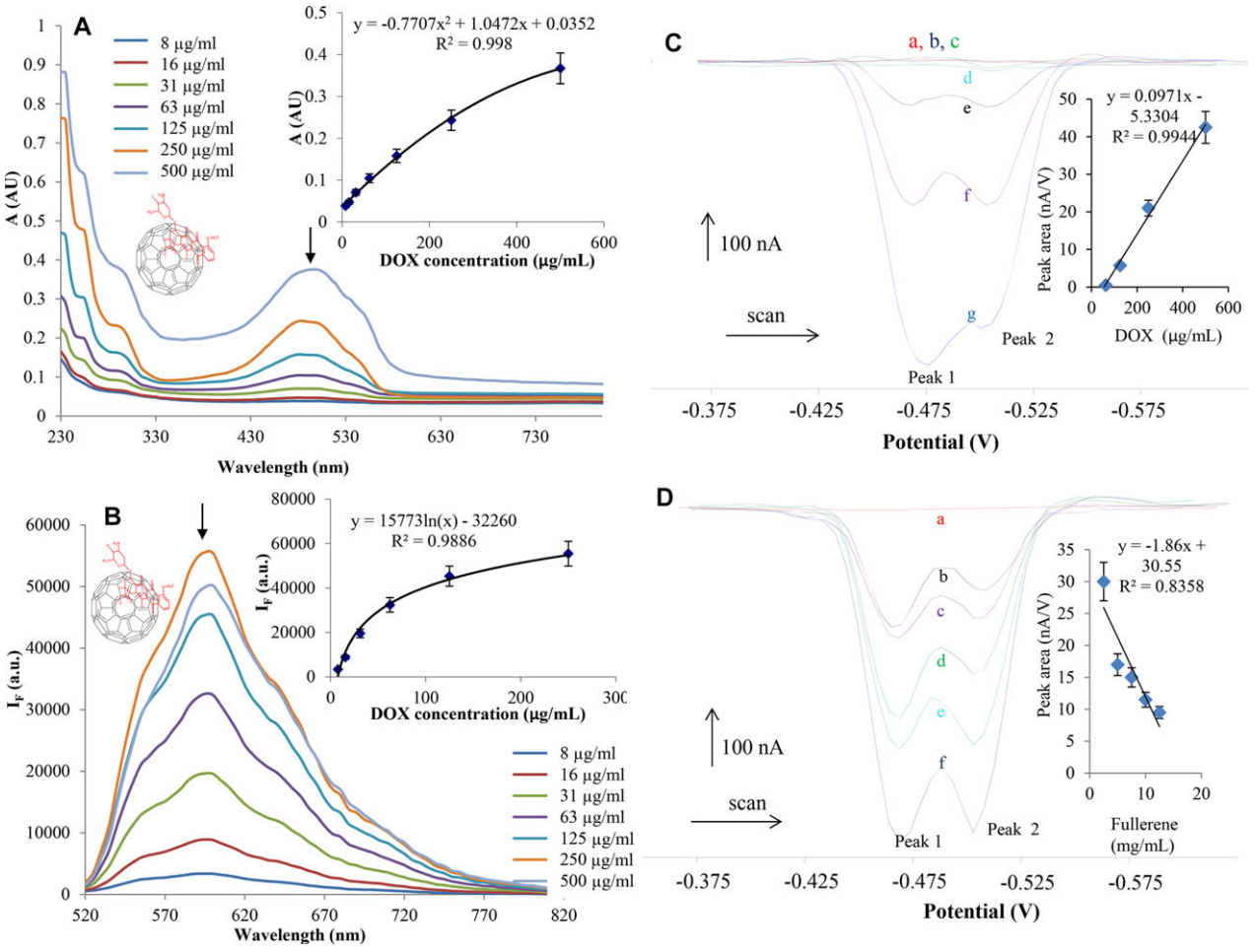

Figure 3. Optical characterization of the prepared conjugates. (A) Absorption spectra of conjugates prepared using constant concentration of fullerenes (5 mg/mL) and varying concentration of DOX (8, 16, 31, 63, 125, 250, and 500 µg/mL), inset: dependence of absorbance on DOX concentration measured at 480 nm. (B) Fluorescence emission spectra of conjugates prepared using constant concentration of fullerenes (5 mg/mL) and varying concentration of DOX (8, 16, 31, 63, 125, 250, and 500 µg/mL), inset: dependence of fluorescence intensity on DOX concentration measured at 600 nm. Electrochemical characterization of the prepared conjugates. (C) Voltammograms of conjugates prepared using constant concentration of fullerenes (5 mg/mL) and varying concentration of DOX (8-a, 16-b, 31-c, 63-d, 125-e, 250-f, and 500-g µg/mL), inset: dependence of the peak area (potential −0.5 V) on DOX concentration. (D) Voltammograms of pure solution of fullerenes (5 mg/mL, a) and conjugates prepared using constant concentration of DOX (500 µg/mL) and varying concentration of fullerenes (2.5-f, 5-e, 7.5-d, 10-c, and 12.5-b mg/mL), inset: dependence of the peak area (potential −0.5 V) on fullerene concentration. All measurements were carried out by square wave voltammetry, parameters were as follows: purging time 120 s; initial potential 0 V; end potential –1.7 V; deposition potential 0.0 V; equilibration time 2 s; time of accumulation 120 s; frequency 150 Hz; step potential 0.005 V; modulation amplitude 0.025 V.

5.9 min under the used HPLC conditions (data not shown). The fact that the signal of pure fullerene solution was not observed under used HPLC conditions using reverse phase and also in the literature the fullerenes are analyzed using different types of separation interactions [37] suggests that the fullerene is retained in the column. Moreover the retention time of DOX and DOX–fullerene conjugates are the same, which supports the hypothesis that the presence of organics in the mobile phase is causing the decomposition of the conjugate and the observed signal belonged to the DOX released from the conjugate. It can be concluded from the results showed in Fig. 4A that the increasing amount of applied DOX led to the increase of the peak height with the retention time of 5.9 min. In the inset of Fig. 5A the dependence of the peak height on the concentration of applied DOX is shown for both electrochemical as well as absorbance detection of HPLC. Both dependences exhibit linear trend with coefficient of determination R^2 of 0.9927 and 0.995, respectively.

On the other hand, analysis by CE-LIF revealed the formation of various complexes of fullerene and DOX (Fig. 4B). Because the fact that the fullerenes do not exhibit fluorescence after the excitation by 488 nm, only conjugates are visualized by this method. The major peak present in the electropherograms is the most abundant complex; however, the formation of other complexes is proved by the presence

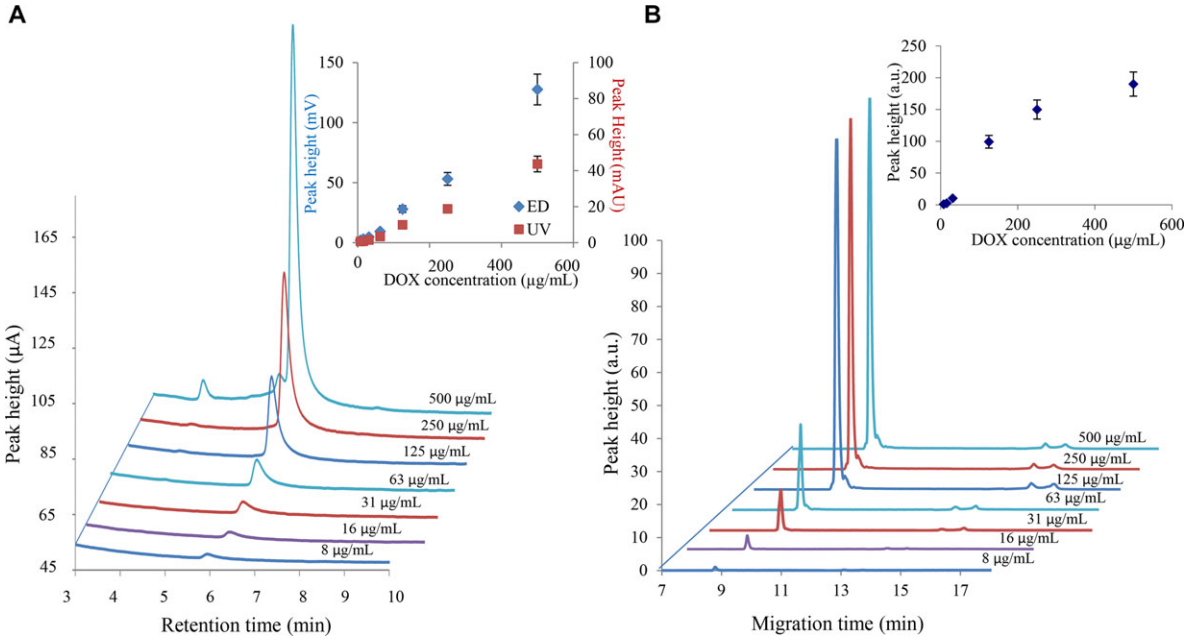

Figure 4. Characterization of DOX–fullerene conjugates by separation techniques. (A) HPLC-ED chromatograms of conjugates prepared using constant concentration of fullerenes (5 mg/mL) and varying concentration of DOX (8, 16, 31, 63, 125, 250, and 500 μg/mL), inset: dependence of the peak height on DOX concentration measured by ED and/or UV detection. (B) Electropherograms measured by CE-LIF of conjugates prepared using constant concentration of fullerenes (5 mg/mL) and varying concentration of DOX (8, 16, 31, 63, 125, 250, and 500 μg/mL); inset: dependence of the peak height on the applied DOX concentration.

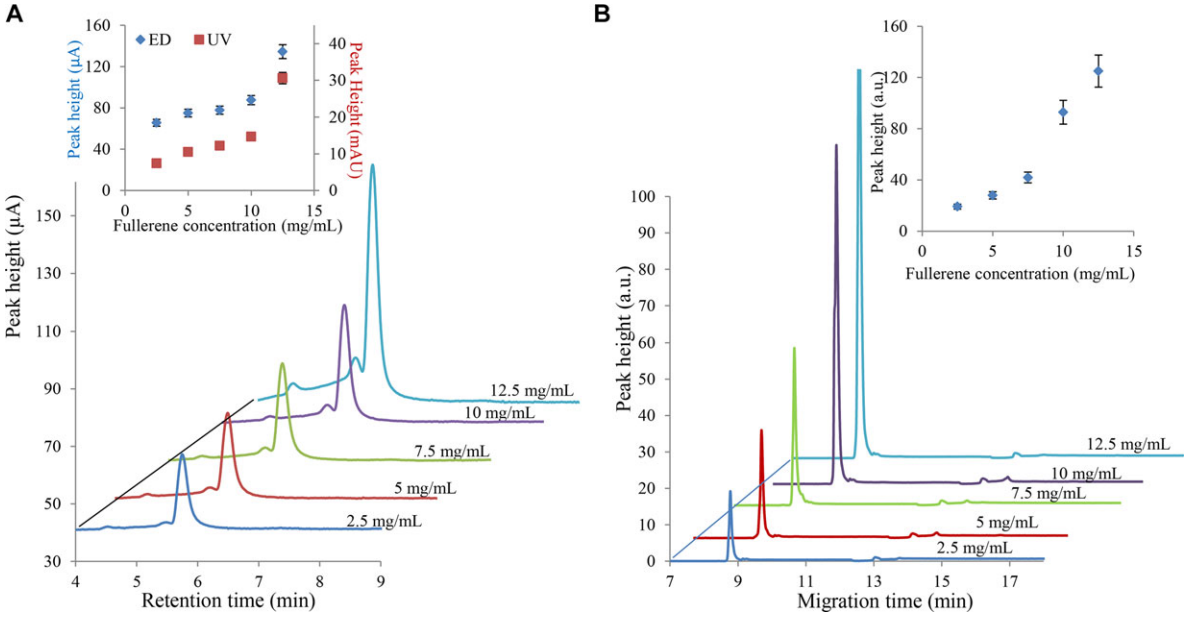

Figure 5. Characterization of DOX–fullerene conjugates by separation techniques. (A) HPLC-ED chromatograms of conjugates prepared using constant concentration of DOX (500 μg/mL) and varying concentration of fullerenes (2.5, 5, 7.5, 10, and 12.5 mg/mL), inset: dependence of the peak height on fullerene concentration measured by ED and UV detection. (B) CE-LIF electropherograms of conjugates prepared using constant concentration of DOX (500 μg/mL) and varying concentration of fullerenes (2.5, 5, 7.5, 10, and 12.5 mg/mL).

of other peaks in the range of 15–17 min with the increasing intensities depending on applied DOX concentration. The dependence of the peak height (major peak) on the concentration of applied DOX is shown in the inset in Fig. 4B. The obtained dependence can be expressed by polynomial equation characterizing the increasing trend of the signal according to concentration of DOX.

Results obtained for the set of solutions prepared using constant concentration of DOX and varying concentration of fullerenes are shown in Fig. 5. Using HPLC an increasing

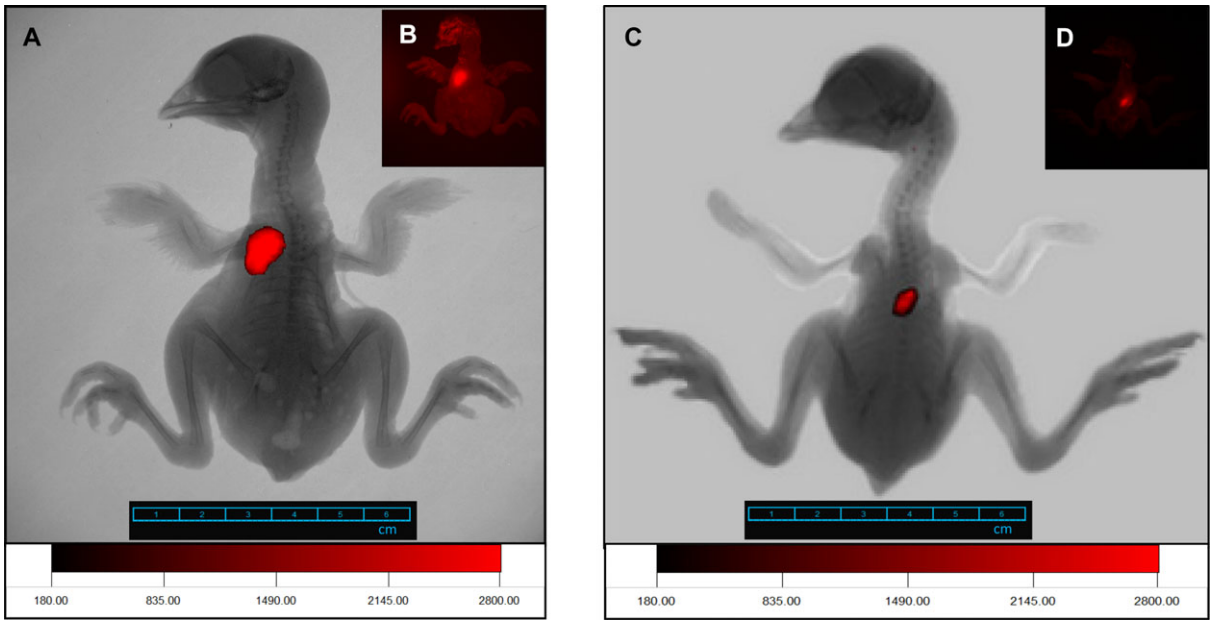

Figure 6. The detection of the DOX in the chicken embryo. Fluorescence monitoring was performed using an In vivo Xtreme system by Carestream. The excitation wavelength was set at 480 nm and the emission was measured at 600 nm. The exposure time 2 s; Binning 2×2 pixels; fStop 1.1; field of view 11.5 × 11.5 cm. (A) Image of chicken embryo (20 days old) administered by DOX–fullerene conjugate (100 μL), overlay of X-ray and fluorescence image, autofluorescence subtracted. (B) Image of chicken embryo administered by DOX–fullerene conjugate, fluorescence image without the subtraction of the autofluorescence. (C) Image of chicken embryo (19 days old) administered by DOX (100 μL), overlay of X-ray and fluorescence image, autofluorescence subtracted. (D) Image of chicken embryo administered by DOX, fluorescence image without the subtraction of the autofluorescence.

trend depending on the increasing the amount of fullerenes is observed (Fig. 5A). As noted previously, the DOX molecules are adsorbed on the fullerene molecules and in the HPLC the DOX is released. This is in agreement with the idea that the increasing amount of fullerenes adsorbs an increasing amount of DOX, which is subsequently released and detected in HPLC. Therefore, the signal of DOX enhanced with the increased concentration of fullerenes as it is shown in the inset in Fig. 5A. The peaks present in chromatograms besides the main peak with migration time of 5.9 min are caused due to the impurities in DOX.

The results for the set of samples prepared using the constant DOX concentration and varying fullerene concentration analyzed by CE-LIF are shown in Fig. 5B. The major peak with migration time of 8.5 min exhibits an increasing signal depending on the increasing concentration of fullerenes. Similarly, the minor peaks with migration time 13–15 min exhibit higher signal in the case of 12.5 mg/mL of fullerenes than in the case of lower concentrations as shown in the inset of the Fig. 5B.

3.5 In vivo sensing of DOX–fullerene conjugates

Finally, behavior of the DOX–fullerene conjugates in the living organism was investigated to verify their great potential for transport and targeted delivery of the cytostatic drugs. Due to the excellent fluorescent properties of DOX, in vivo imaging observation is possible [22]. Moreover, as mentioned, fullerenes exhibit protective properties against the toxic effect of the DOX. The chicken embryo was taken out of the eggshell and the DOX or DOX–fullerene conjugate was applied into the breast muscle tissue, the feather was removed and the autofluorescence of muscle tissue was eliminated by software. Due to the good fluorescence properties of the DOX, it was possible to observe the distribution of DOX–fullerenes in muscle tissues. Fluorescence detected in the chicken using pure DOX solution (100 μL, 500 μg/mL) injected into the 5 mm under the skin is shown in Fig. 6A. The mean fluorescence intensity of DOX was 6549 a.u. The fluorescence image is shown in Fig. 6B—showing besides the signal of DOX also the autofluorescence of the muscle tissue. In Fig. 6C, the chicken embryo administered by the DOX–fullerene conjugates (100 μL, 500 μg/mL DOX, and 5 mg/mL fullerenes) is shown to demonstrate the possibility of the conjugates to be detected by the in vivo system. The mean fluorescence intensity of the conjugates was 5849 a.u. The fluorescence intensity of conjugates was lower compared to pure DOX due to the incomplete conjugation onto the fullerene surface.

Furthermore, the DOX–fullerenes conjugates (250 μL) prepared by the constant concentration of fullerenes (5 mg/mL) and varying concentration of DOX (31, 63, 125, 250, and 500 μg/mL) were administered into the egg yolk of the five specimens of 17 day-old chicken embryos and incubated for 4 h to enable the distribution of the DOX–fullerene conjugates into the embryo. After the desired time the embryos were extracted and the discrete organs (heart, brain, liver, and intestine) were analyzed using HPLC to determine

Table 1. Quantification of DOX supplied in the form of DOX–fullerene conjugates (with varying DOX concentration) accumulated in particular organ of the chicken embryo

		DOX–fullerene		
		Concentration (μg/g)	Sum (μg/g)	Average (μg/g)
500 μg/mL	Brain	1.1	32.2	8.05
	Heart	5.5		
	Liver	3.6		
	Intestine	22.0		
250 μg/mL	Brain	0.5	7.3	1.8
	Heart	3.5		
	Liver	1.1		
	Intestine	2.2		
125 μg/mL	Brain	0.5	2.7	0.7
	Heart	0.8		
	Liver	0.6		
	Intestine	0.8		
63 μg/mL	Brain	0.3	2.7	0.7
	Heart	0.7		
	Liver	1.1		
	Intestine	0.6		
31 μg/mL	Brain	0.4	1.3	0.3
	Heart	0.9		
	Liver	ND		
	Intestine	ND		

the DOX amount. The DOX amount in the organs, the average and total (sum) amount determined per each chicken is summarized in Table 1. As expected the total (sum) and average DOX amount is decreasing depending on the concentration of DOX applied to the preparation process of conjugates. However, within one chicken the DOX amount varied depending on the analyzed organ. Generally, in all studied chicken embryos the highest DOX concentration was determined in the intestine followed by heart and liver.

4 Concluding remarks

The DOX is effective cytostatics, however, exhibiting severe side effect, which can be eliminated by number of approaches [38]. One of them is the conjugation with fullerenes, which have proven to have protective properties against the DOX toxicity. Concurrently, fullerenes increase the size of the DOX molecule and therefore the time before the drug is eliminated from the organism is prolonged. In this study, we demonstrated the conjugation procedure for formation of the DOX–fullerene complexes and their characterization by optical and electrochemical method. Finally, in vivo monitoring of the conjugates in the chicken embryos was performed investigating their distribution in the particular organs of the chicken embryo.

Financial support from CYTORES GA CR P301/10/0356 (EA 14) and CEITEC CZ.1.05/1.1.00/02.0068 is highly acknowledged.

The authors have declared no conflict of interest.

5 References

[1] Dunk, P. W., Kaiser, N. K., Hendrickson, C. L., Quinn, J. P., Ewels, C. P., Nakanishi, Y., Sasaki, Y., Shinohara, H., Marshall, A. G., Kroto, H. W., *Nat. Commun.* 2012, *3*, 855.

[2] Rogers, J. A., Lagally, M. G., Nuzzo, R. G., *Nature* 2011, *477*, 45–53.

[3] Guo, F. W., Yang, B., Yuan, Y. B., Xiao, Z. G., Dong, Q. F., Bi, Y., Huang, J. S., *Nat. Nanotechnol.* 2012, *7*, 798–802.

[4] Popov, A. A., Yang, S. F., Dunsch, L., *Chem. Rev.* 2013, *113*, 5989–6113.

[5] Ji, S. R., Liu, C., Zhang, B., Yang, F., Xu, J., Long, J. A., Jin, C., Fu, D. L., Ni, Q. X., Yu, X. J., *Biochim. Biophys. Acta-Rev. Cancer* 2010, *1806*, 29–35.

[6] Pumera, M., *Curr. Drug Metab.* 2012, *13*, 251–256.

[7] Chen, Z. Y., Mao, R. Q., Liu, Y., *Curr. Drug Metab.* 2012, *13*, 1035–1045.

[8] Injac, R., Perse, M., Boskovic, M., Djordjevic-Milic, V., Djordjevic, A., Hvala, A., Cerar, A., Strukej, B., *Technol. Cancer Res. Treat.* 2008, *7*, 15–25.

[9] Jacevic, V., Djordjevic-Milic, V., Dragojevic-Simic, V., Radic, N., Govedarica, B., Dobric, S., Srdjenovic, B., Injac, R., Djordjevic, A., Vasovic, V., *Toxicol. Lett.* 2007, *172*, S146–S146.

[10] Milic, V. D., Djordjevic, A., Dobric, S., Injac, R., Vuckovic, D., Stankov, K., Simic, V. D., Suvajdzic, L., in: Uskokovic, D. P., Milonjic, S. K., Rakovic, D. I. (Eds.), *Recent Developments in Advanced Materials and Processes*, Trans Tech Publications Ltd, Zurich-Uetikon 2006, pp. 525–529.

[11] Icevic, I. D., Vukmirovic, S. N., Srdenovic, B. U., Sudji, J. J., Djordjevic, A. N., Injac, R. M., Vasovic, V. M., *Hem. Ind.* 2011, *65*, 329–337.

[12] Li, X. H., Zhang, C., Le Guyader, L., Chen, C. Y., *Sci. China-Chem.* 2010, *53*, 2241–2249.

[13] Liu, J. H., Cao, L., Luo, P. J. G., Yang, S. T., Lu, F. S., Wang, H. F., Meziani, M. J., Haque, S. A., Liu, Y. F., Lacher, S., Sun, Y. P., *ACS Appl. Mater. Interfaces* 2010, *2*, 1384–1389.

[14] Zakharian, T. Y., Seryshev, A., Sitharaman, B., Gilbert, B. E., Knight, V., Wilson, L. J., *J. Am. Chem. Soc.* 2005, *127*, 12508–12509.

[15] Kizek, R., Adam, V., Hrabeta, J., Eckschlager, T., Smutny, S., Burda, J. V., Frei, E., Stiborova, M., *Pharmacol. Ther.* 2012, *133*, 26–39.

[16] Bogdanovic, G., Kojic, V., Dordevic, A., Canadanovic-Brunet, J., Vojinovic-Miloradov, M., Baltic, V. V., *Toxicol. Vitro* 2004, *18*, 629–637.

[17] Injac, R., Perse, M., Cerne, M., Potocnik, N., Radic, N., Govedarica, B., Djordjevic, A., Cerar, A., Strukelj, B., *Biomaterials* 2009, *30*, 1184–1196.

[18] Heister, E., Neves, V., Tilmaciu, C., Lipert, K., Beltran, V. S., Coley, H. M., Silva, S. R. P., McFadden, J., *Carbon* 2009, *47*, 2152–2160.

[19] Ali-Boucetta, H., Al-Jamal, K. T., McCarthy, D., Prato, M., Bianco, A., Kostarelos, K., *Chem. Commun.* 2008, *2008*, 459–461.

[20] Chaudhuri, P., Paraskar, A., Soni, S., Mashelkar, R. A., Sengupta, S., *ACS Nano* 2009, *3*, 2505–2514.

[21] Liu, Z., Sun, X. M., Nakayama-Ratchford, N., Dai, H. J., *ACS Nano* 2007, *1*, 50–56.

[22] Blazkova, I., Vaculovicova, M., Eckschlager, T., Stiborova, M., Trnkova, L., Adam, V., Kizek, R., *Chem. Sensors* 2014, *4*, 9.

[23] Lu, F. S., Haque, S. A., Yang, S. T., Luo, P. G., Gu, L. R., Kitaygorodskiy, A., Li, H. P., Lacher, S., Sun, Y. P., *J. Phys. Chem. C* 2009, *113*, 17768–17773.

[24] Fernandez-Saiz, P., Soler, C., Lagaron, J. M., Ocio, M. J., *Int. J. Food Microbiol.* 2010, *137*, 287–294.

[25] Borneman, D. L., Ingham, S. C., Ane, C., *J. Food Prot.* 2009, *72*, 1190–1200.

[26] Rufian-Henares, J. A., Morales, F. J., *Food Chem.* 2008, *111*, 1069–1074.

[27] Hevia, D., Rodriguez-Garcia, A., Cimadevilla, H. M., Mayo, J. C., *Eur. J. Cancer* 2012, *48*, S246–S246.

[28] Huska, D., Adam, V., Babula, P., Hrabeta, J., Stiborova, M., Eckschlager, T., Trnkova, L., Kizek, R., *Electroanalysis* 2009, *21*, 487–494.

[29] Huska, D., Adam, V., Burda, J., Hrabeta, J., Eckschlager, T., Babula, P., Opatrilova, R., Trnkova, L., Stiborova, M., Kizek, R., *Febs J.* 2009, *276*, 109–109.

[30] Hynek, D., Krejcova, L., Zitka, O., Adam, V., Trnkova, L., Sochor, J., Stiborova, M., Eckschlager, T., Hubalek, J., Kizek, R., *Int. J. Electrochem. Sci.* 2012, *7*, 13–33.

[31] Hynek, D., Krejcova, L., Zitka, O., Adam, V., Trnkova, L., Sochor, J., Stiborova, M., Eckschlager, T., Hubalek, J., Kizek, R., *Int. J. Electrochem. Sci.* 2012, *7*, 34–49.

[32] Masarik, M., Krejcova, L., Hynek, D., Adam, V., Stiborova, M., Eckschlager, T., Kizek, R., *Int. J. Mol. Med.* 2012, *30*, S45–S45.

[33] Morita, T., Lindsay, S., *J. Phys. Chem. B* 2008, *112*, 10563–10572.

[34] Park, B. K., Lee, G., Kim, K. H., Kang, H., Lee, C. Y., Miah, M. A., Jung, J., Han, Y. K., Park, J. T., *J. Am. Chem. Soc.* 2006, *128*, 11160–11172.

[35] Winkler, K., Balch, A. L., Kutner, W., *J. Solid State Electrochem.* 2006, *10*, 761–784.

[36] Winkler, K., Costa, D. A., Balch, A. L., *Pol. J. Chem.* 2000, *74*, 1–37.

[37] Coutant, D. E., Clarke, S. A., Francis, A. H., Meyerhoff, M. E., *J. Chromatogr. A* 1998, *824*, 147–157.

[38] Blazkova, I., Nguyen, V. H., Dostalova, S., Kopel, P., Stanisavljevic, M., Vaculovicova, M., Stiborova, M., Eckschlager, T., Kizek, R., Adam, V., *Int. J. Mol. Sci.* 2013, *14*, 13391–13402.

